

1 **Supplementary Figure legends**

2 **Fig. S1** (A) PCA (Principal Component Analysis) of transcriptomic data from normal,  
3 AP and SAP C57BL/6 mouse samples. (B) Volcano plot showing the differentially  
4 expressed genes between AP model mice and normal controls and between SAP  
5 model mice and normal controls. (C) Hierarchical clustering analyses identified 4  
6 major expression modules from the transcriptomic analysis. (D) KEGG analysis of  
7 the pathways enriched in SAP vs. AP using transcriptomic analysis. (E) PCA of  
8 proteomic data from normal, AP and SAP samples from C57BL/6 mice. (F) KEGG  
9 analysis of the enriched in the differentially expressed proteins between SAP and AP  
10 model mice using proteomic data. (G) Integrative analysis of transcriptomic and  
11 proteomic data and 1400 DEGs that coexisted between the AP vs. control group and  
12 802 between the SAP vs. control group. (H) List of coexisting genes that were  
13 significantly upregulated in AP but downregulated in SAP. (I) List of coexisting genes  
14 that were significantly downregulated in AP but upregulated in SAP.

15 **Fig. S2** (A) Representative images of Ly6G (green) in WT and Hspb1 KO mice  
16 generated by 8 hourly injections of caerulein. Scale bar, 50  $\mu$ m. (B) Schematic of the  
17 process of establishing SAP models using mice via AAV8 administration. (C)  
18 Amylase and lipase activity in the plasma of the AAV8-con and AAV8-Hspb1 groups  
19 in the caerulein-induced SAP model. n=5. (D-E) Representative images and  
20 statistical analysis of Ly6G or CD68 (green) expression in the pancreas between the  
21 AAV8-ctrl and AAV8-Hspb1 groups in caerulein-induced SAP (n=5). Scale bar, 50  
22  $\mu$ m. (F) Flow cytometry analysis of blood parameters in the AAV8-ctrl and AAV8-  
23 Hspb1 groups in the duct ligation-induced SAP model. Ctrl, control. \*\*p<0.01.

24 **Fig. S3** (A) Representative images and statistical analysis of cleaved caspase 3  
25 expression in the pancreas according to IHC staining between WT and Hspb1 KO  
26 mice with caerulein-induced AP (n=5). Scale bar, 100  $\mu$ m. (B) Western blot analysis

27 and corresponding statistical analysis, comparing the expression of cleaved caspase  
28 3 between WT and Hspb1 KO mice with caerulein-induced AP (n=5). (C)  
29 Representative images and statistical analysis of cleaved caspase 3 expression in  
30 the pancreas according to IHC staining in the AAV8-ctrl and AAV8-Hspb1 groups of  
31 patients with caerulein-induced SAP (n=5). Scale bar, 100  $\mu$ m. (D) Western blot  
32 analysis and corresponding statistical analysis, comparing the expression of cleaved  
33 caspase 3 between the AAV8-ctrl and AAV8-Hspb1 mice with caerulein-induced AP  
34 (n=5). (E-G) Representative images of IHC staining, Western blot and statistical  
35 analysis of SLC3A2 and SLC7A11 expression in the pancreas between WT and  
36 Hspb1 KO mice with caerulein-induced AP (n=5). Scale bar, 100  $\mu$ m. \* $p$ <0.5;  
37 \*\*\* $p$ <0.001.

38 **Fig. S4** (A-B) Representative images of IHC staining, Western blot and statistical  
39 analysis of Anxa2 expression in the pancreas between WT and Hspb1 KO mice with  
40 caerulein-induced AP (n=5). Scale bar, 100  $\mu$ m. (C-D) Representative images of IHC  
41 staining, Western blot and statistical analysis of Anxa2 expression in the pancreas  
42 between the AAV8-ctrl and AAV8-Hspb1 groups in SAP patients (n=5). Scale bar, 100  
43  $\mu$ m. (E-F) Representative images of IHC staining, Western blot and statistical  
44 analysis of p-Anxa2 expression in the pancreas of normal, WT and Hspb1-KO mice  
45 with caerulein-induced AP (n=5). Scale bar, 100  $\mu$ m. WT, wild type; KO, Anxa2 KO.  
46 \* $p$ <0.5, \*\* $p$ <0.01, \*\*\* $p$ <0.001.

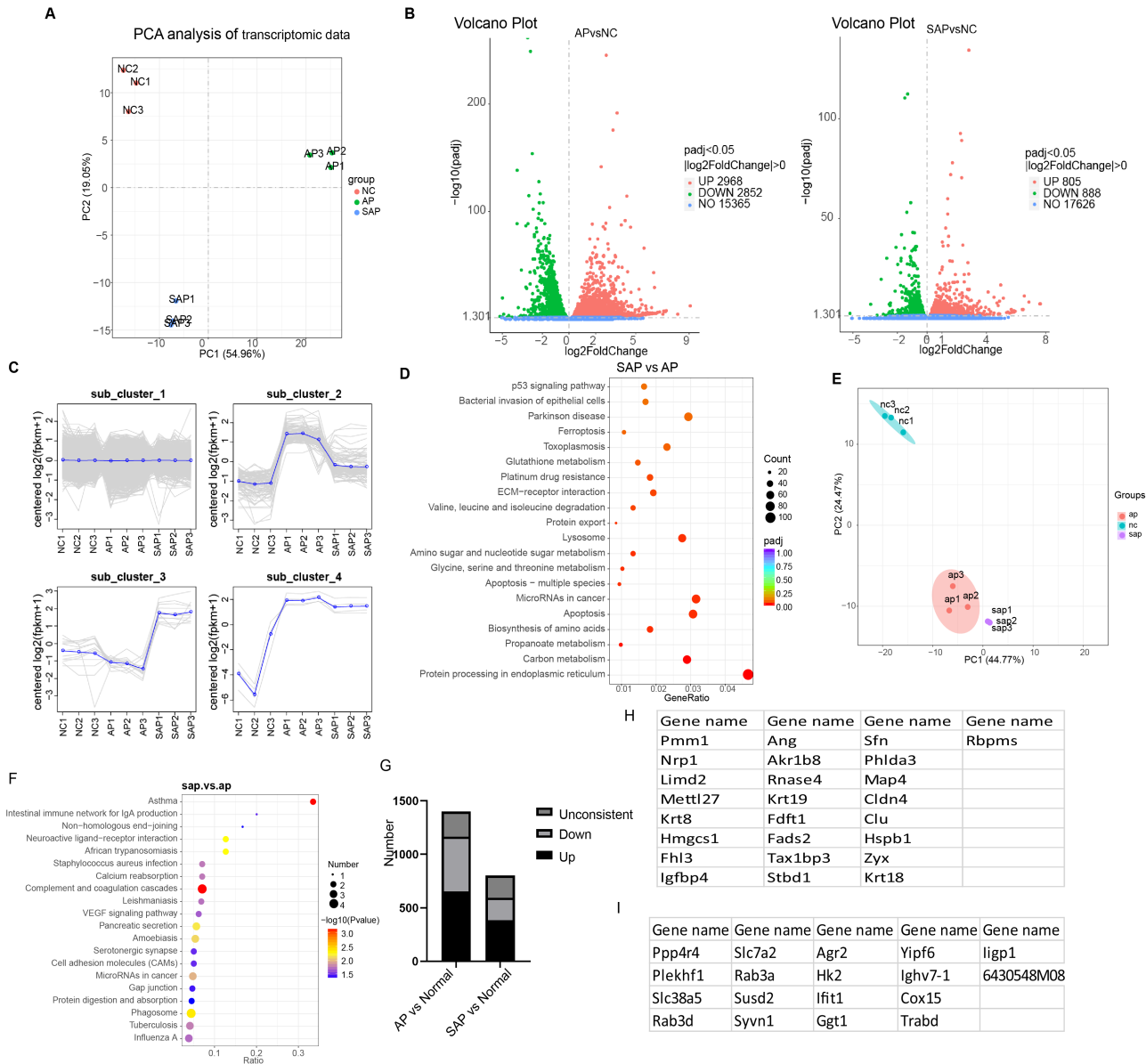
47 **Fig. S5** (A) Schematic diagram describing the strategy used to establish Anxa2 KO  
48 mice. (B-C) H&E staining and statistical analysis were performed to evaluate the  
49 pancreatic tissue of WT and Anxa2 KO mice treated with or without AAV8-Hspb1  
50 (n=5-6). Scale bar, 100  $\mu$ m. (D) Amylase and lipase activity in the plasma of WT and  
51 Anxa2 KO mice treated with or without AAV8-Hspb1 (n=5-6). (E) 266-6 cells were  
52 pretreated as indicated. Representative images and statistical analysis of the  
53 fluorescence signal at a 594 nm wavelength after incubation with 5  $\mu$ M DHE for 10

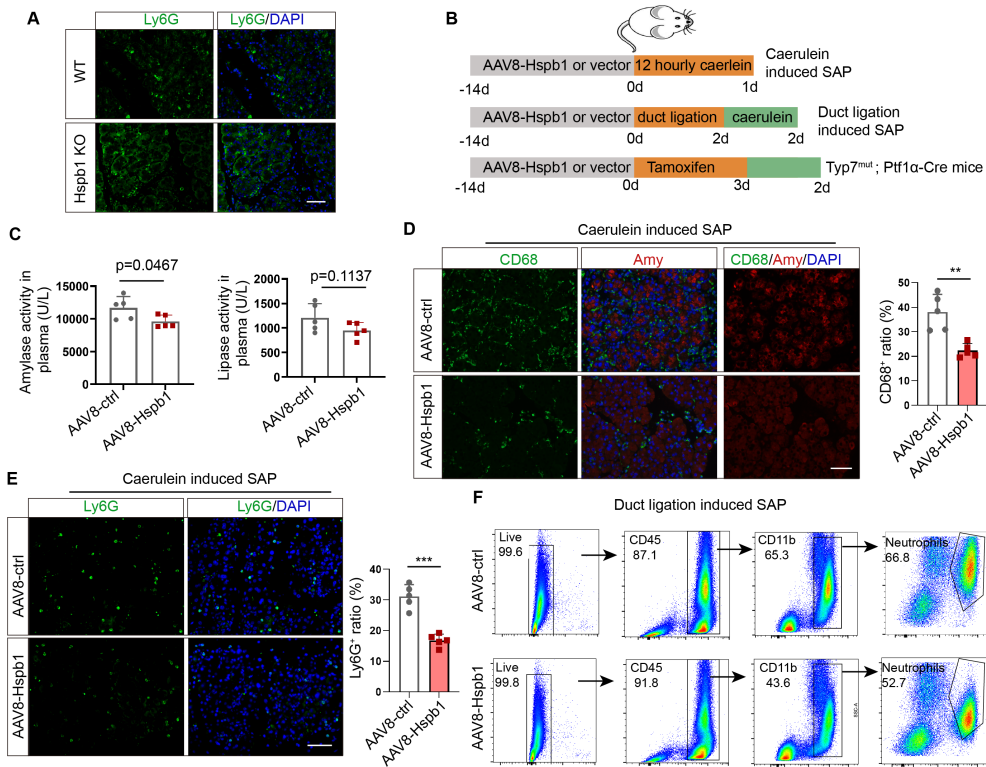
54 min. Scale bar, 50  $\mu$ m. (F) Representative images and statistical analysis of the  
55 fluorescence signal at a 488 nm wavelength after incubation with 2.5  $\mu$ M BODIPY  
56 581/591 C11 for 30 min. Scale bar, 50  $\mu$ m. NC, negative control; TAC, taurocholate  
57 acid; oe, overexpression; si, siRNA; WT, wild type; KO, Anxa2 KO. \* $p$ <0.5, N.S., not  
58 significant; \*\*\* $p$ <0.001.

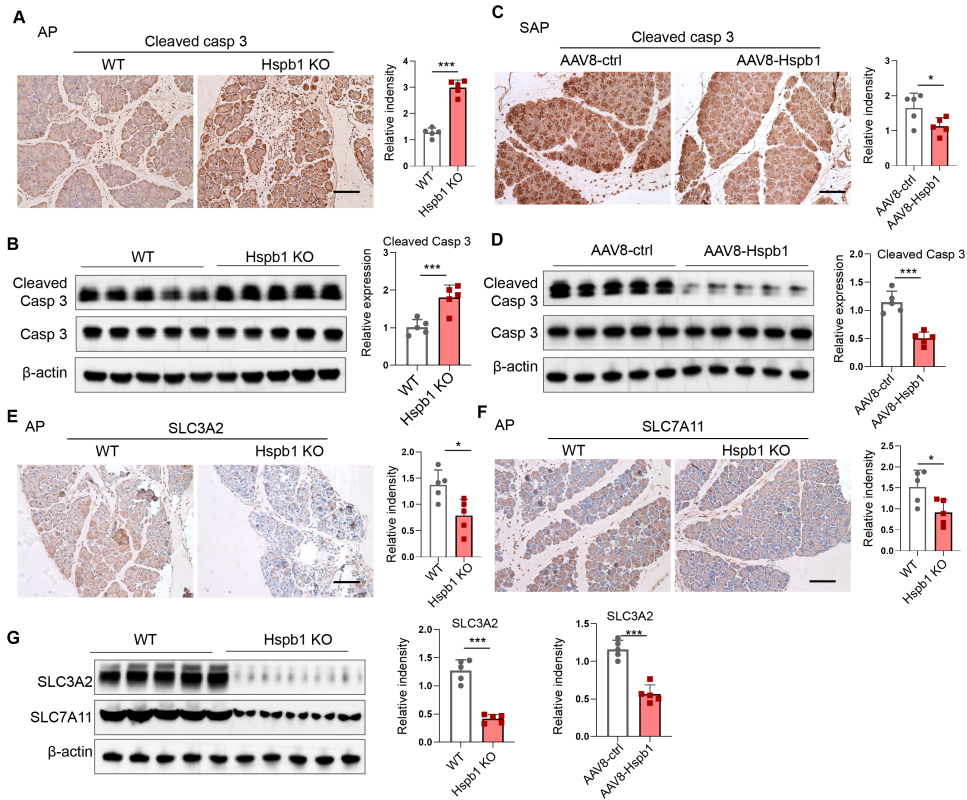
59 **Fig. S6** (A-C) Representative images of IHC staining, Western blot and statistical  
60 analysis of pancreatic Prdx1 and p-Prdx1 expression in WT and Hspb1-KO mice with  
61 caerulein-induced AP (n=5). Scale bar, 100  $\mu$ m. (D-F) Representative images of IHC  
62 staining, Western blot and statistical analysis of Prdx1 and p-Prdx1 expression in the  
63 pancreas in the AAV8-ctrl and AAV8-Hspb1 groups of SAP patients (n=5). Scale bar,  
64 100  $\mu$ m. \* $p$ <0.5, N.S., not significant; \*\* $p$ <0.01.

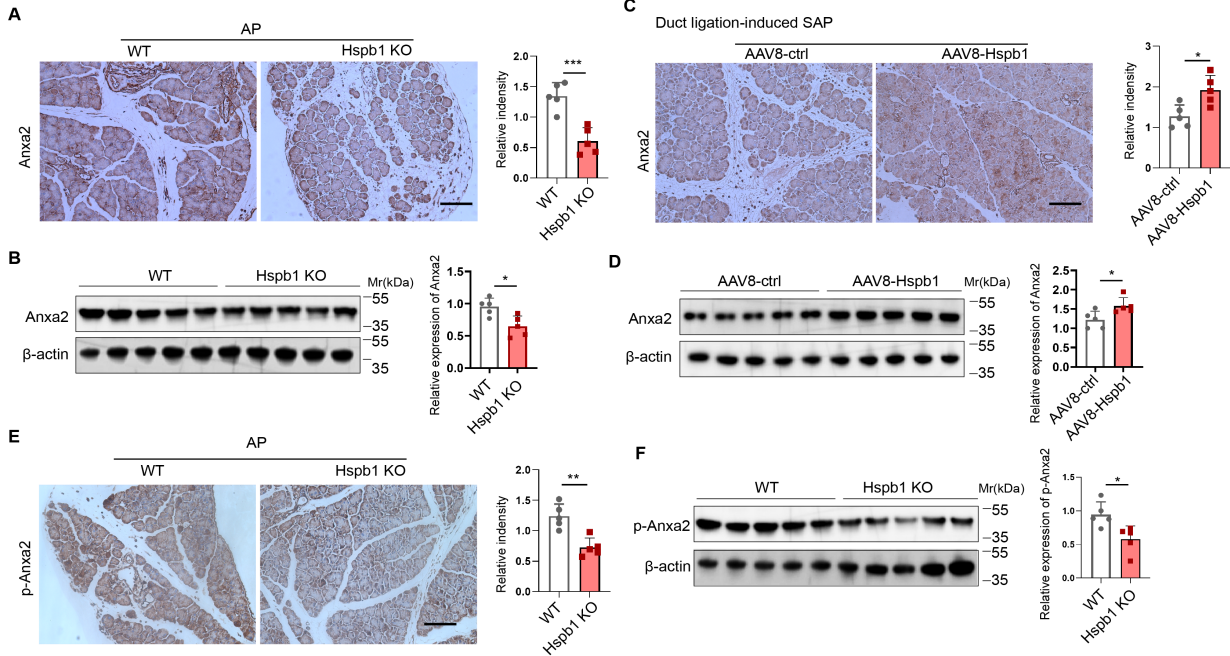
65

# Fig. S1



**Fig. S2**

**Fig. S3**

**Fig. S4**

# Fig. S5

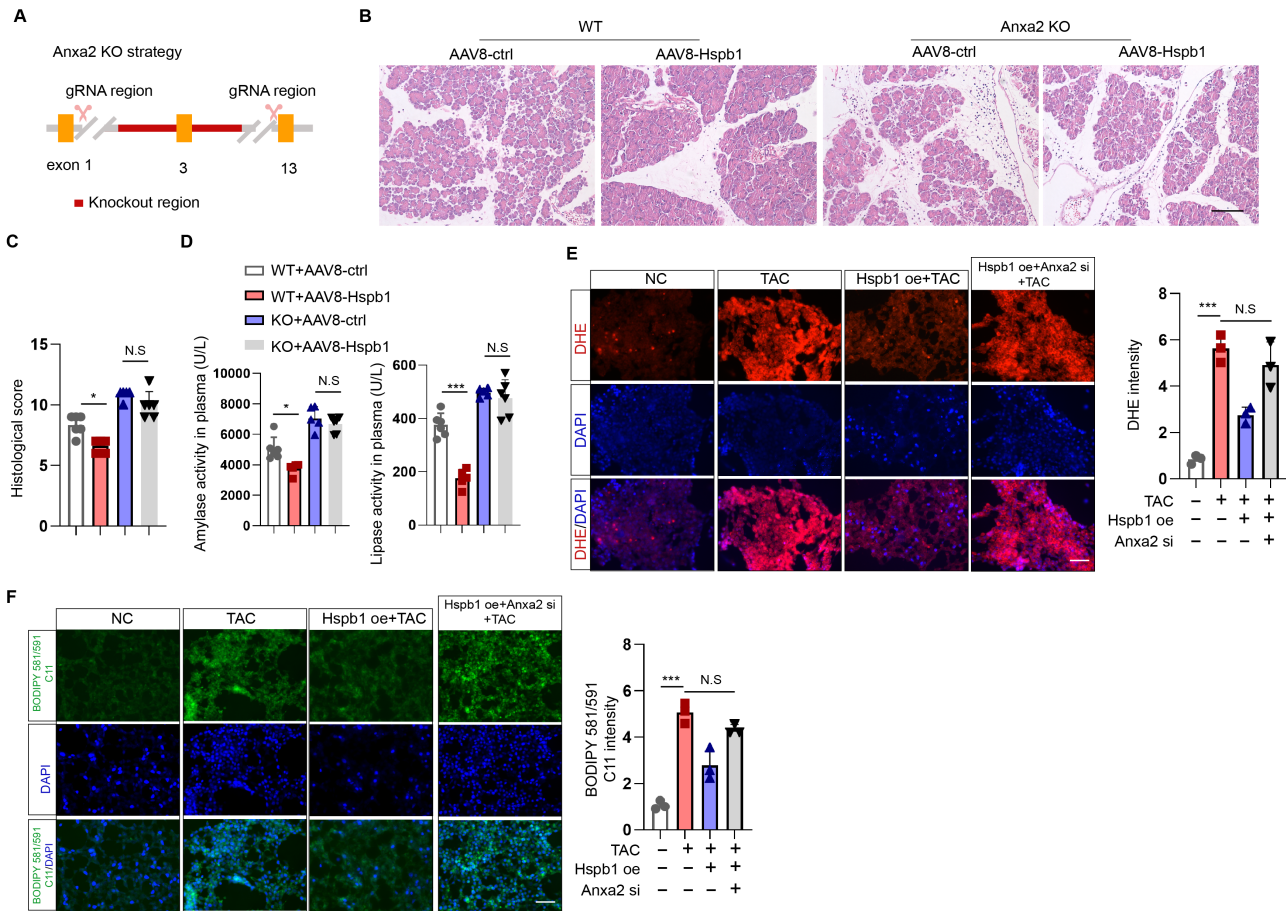




**Fig. S6**